Journal of Alloys and Compounds 509 (2011) 4854–4860

Contents lists available at ScienceDirect

Journal of Alloys and Compounds

journal homepage: www.elsevier.com/locate/jallcom

Annealing behaviour of Mg–3Al–1Zn alloy sheet obtained by a combination of high-temperature rolling and subsequent warm rolling

Xinsheng Huang*, Kazutaka Suzuki, Yasumasa Chino

Materials Research Institute for Sustainable Development, National Institute of Advanced Industrial Science and Technology (AIST), Nagoya, Aichi 463-8560, Japan

ARTICLE INFO

Article history:
Received 29 October 2010
Received in revised form 22 January 2011
Accepted 27 January 2011
Available online 23 February 2011

Keywords:
Magnesium alloy
Recrystallization
Grain growth
Microstructure
Texture

ABSTRACT

The recrystallization and grain growth behaviour of Mg–3Al–1Zn alloy sheets with a deformation microstructure, obtained by a combination of high-temperature rolling and subsequent warm rolling, was investigated at different stages of annealing. The basal texture was significantly weakened as a result of the formation of new grains with a largely altered *c*-axis orientation relative to the initial basal orientation owing to discontinuous static recrystallization during primary recrystallization. The new grains nucleated mostly at the pre-existing grain boundaries rather than at the intersections of twins or within the twins. Subsequent grain growth led to further progression of the texture weakening accompanied by an enhancement in the basal pole inclination.

1. Introduction

In the study of magnesium (Mg) alloys, a large amount of effort has been devoted to dynamic crystallization (DRX) studies, e.g. investigation of the influence of thermomechanical parameters on the DRX grain size [1] and elucidation of the DRX mechanism [2], owing to the fact that DRX leads to grain refinement during deformation and, in turn, to enhancements of hot workability and mechanical properties. In contrast, little work has been done on static recrystallization (SRX) during annealing after deformation especially on the texture evolution and elucidation of the mechanism of SRX in wrought Mg alloys. The lack of information on SRX may be related to the fact that the basal texture, which is detrimental to formability, cannot be changed markedly by annealing, in most cases [3–12]. The final annealing texture is dominated by primary recrystallization and grain growth. It is generally observed that, in wrought Mg alloys, there is a slight weakening of the texture during initial recrystallization, followed by the development of basal texture during subsequent grain growth [13]. In addition, recrystallization and particularly grain growth tend to result in a single peak replacing a double peak in the basal pole during annealing [5,7]. Yang et al. [3,4] reported that annealing mainly results in grain coarsening accompanied by a scarcely changed texture, i.e. continuous SRX, in the case of hot deformed Mg–3Al–1Zn (AZ31) alloy with a continuous DRXed microstructure. Twins generally play an important role during SRX and may serve as nucleation sites. Yi et al. [9] reported that new grains are formed at the intersections of two double twins but the orientation of new grains is characterized by a rotation around the *c*-axis with respect to the matrix grains, which leads to persistence of a strong basal texture. Even though new grains forming within compression twins exhibit non-basal orientation, the deformation texture is retained because of the restricted growth of the new grains formed from the compression twins into the matrix grains [10]. Particle-stimulated nucleation (PSN) may occur in Mg alloys containing second-phase particles with sizes larger than about 1 μm, and new grains induced by PSN tend to exhibit random orientations [13–16]. However, the influence of PSN on the overall texture is generally quite weak in most Mg alloys, including the most common wrought Mg alloy (i.e. AZ31 alloy) because these alloys contain small amounts of second-phase particles [13,16,17]. Addition of rare-earth (RE) elements is an effective way to weaken the texture and split the basal pole largely, resulting in remarkable improvements in the formability of Mg alloys. This texture favoured for deformation results from solute effects and possibly combined with the PSN effects [18,19]. Nonetheless, the addition of RE elements substantially increases the cost of the raw material. Recently, a significantly weakened texture with a largely tilted basal pole was achieved by annealing of an AZ31 alloy sheet obtained by a combination of high-temperature rolling and subsequent warm rolling, which led to a superior stretch formability comparable to aluminium alloys [20]. This anomalous

* Corresponding author at: Materials Research Institute for Sustainable Development, National Institute of Advanced Industrial Science and Technology, 2266-98 Anagahora, Shimo-Shidami, Moriyama-ku, Nagoya, Aichi 463-8560, Japan.
Tel.: +81 52 736 7088; fax: +81 52 736 7406.
E-mail address: huang-xs@aist.go.jp (X. Huang).

0925-8388/$ – see front matter © 2011 Elsevier B.V. All rights reserved.
doi:10.1016/j.jallcom.2011.01.189

annealing texture implies that the annealing behaviour is different from those mentioned above, and it is therefore important to reveal it from the viewpoint of both scientific and industrial significances. In this study, the microstructural and textural evolution of the AZ31 alloy sheet with the superior stretch formability was investigated at different stages of annealing.

2. Experimental

The rolling procedure of the AZ31 alloy sheet used for the investigation has been described previously [20]. In short, the sheet was processed by three-pass differential speed rolling with a rotation speed ratio of 1.36 at a high temperature of 823 K, followed by final warm rolling at 498 K with a thickness reduction per pass of 33%. Both rolls were heated to 498 K or 573 K when the billet temperature was 498 K or 823 K, respectively. The DRXed microstructure of the sheet rolled at 823 K for three passes (i.e. the state prior to the final warm rolling) was characterized by a relatively weak basal texture intensity of 4.8 and a large grain size of 18 μm, which was attributed to the effects of high temperature rolling [21]. The macro- and micro-textures were investigated using the Schulz reflection method and electron backscattered diffraction (EBSD), respectively. The macro-textures were investigated at the mid-layer of the sheet. The EBSD analyses were carried out at the central region of the longitudinal section, and the rotation of the orientation was conducted in order to obtain the same observation direction as that of the macro textures. The sample preparation method for the EBSD analyses was the same as that reported previously in Ref. [22]. Transmission electron microscope (TEM) was used to observe the substructure of the as-rolled sheet.

3. Results and discussion

The microstructures and the (0 0 0 2) pole figures of the as-rolled sheet together with those of the sheets annealed at 523 K and 773 K for 3.6×10^3 s are shown in Fig. 1(a–c), and the changes in the basal texture intensity and grain size with increasing annealing temperature are shown in Fig. 1(d). The as-rolled sheet exhibits a strong basal texture with a deformation microstructure including twins and deformed grains. There is no indication of the occurrence of DRX, which results from the microstructure with a relatively weak texture and coarse grains prior to final warm rolling [20]. Annealing at 523 K results in the completion of SRX, and the basal texture intensity weakens significantly from 7.9 to 4.3. At this annealing stage, almost no change occurs in the inclination angle of the basal pole, which remains at ~12°, close to that (~10°) of the as-rolled sheet, as indicated by the arrows in the (0 0 0 2) pole figures. As the annealing temperature is increased from 523 K to 773 K, the change in the microstructure is dominated by grain growth, which increases the grain size from 8 μm to 21 μm. It is interesting to note that the basal texture intensity weakens further from 4.3 to 2.7 and the inclination of the basal pole toward the rolling direction (RD) is also enhanced from ~12° to ~25° as grain coarsening progresses. These phenomena are opposite to those generally observed in pure Mg and its alloys, in which the grain growth tends to induce strengthening of the basal texture and disappearance of the basal pole inclination [5–7,23].

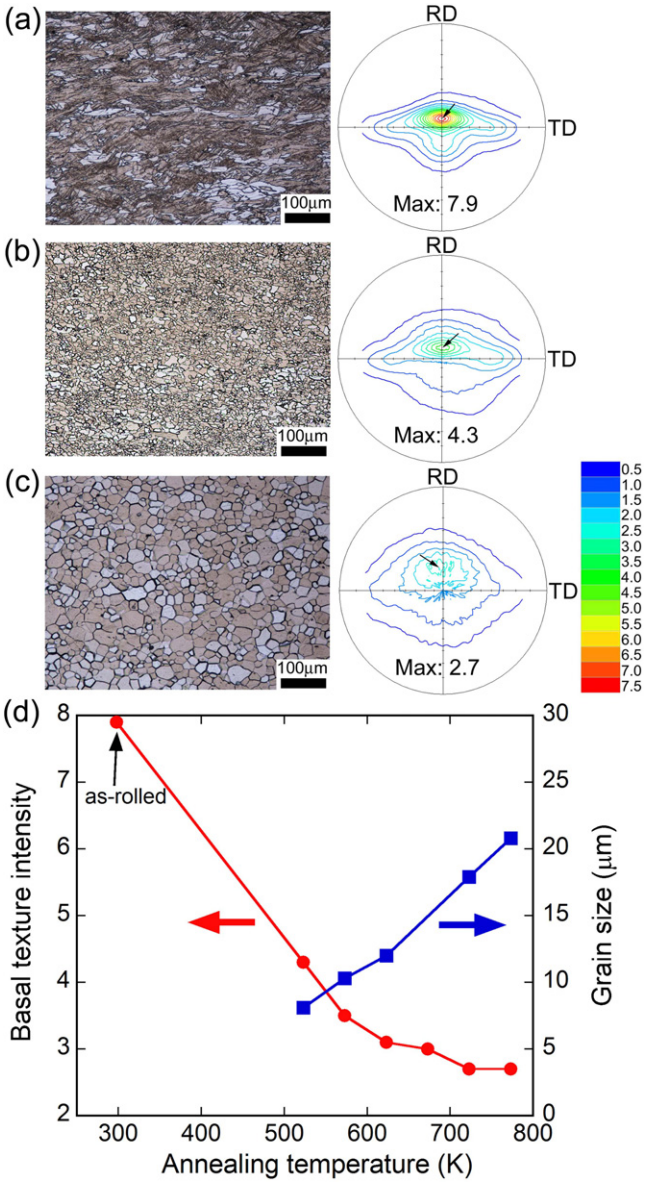

Fig. 1. Optical micrographs for longitudinal section with horizontal RD and (0 0 0 2) pole figures (intensity levels: 0.5, 1, 1.5, etc.) of (a) as-rolled sheet [20] together with sheets annealed at (b) 523 K and (c) 773 K for 3.6×10^3 s. (d) Basal texture intensity and grain size as function of annealing temperature (hold time: 3.6×10^3 s). The arrows indicate the maxima of the (0 0 0 2) pole figures.

Fig. 2 shows the inverse pole figure maps, the (0 0 0 1) and $(1\,0\,\bar{1}\,0)$ pole figures, together with the distributions of the grain boundary misorientation of the as-rolled sheet and the sheets annealed under various conditions. The rolling texture exhibits a strong basal fiber and a large spread of the (0 0 0 1) orientation in the transverse direction (TD). The low image quality (IQ) of the as-rolled specimen is due to a large residual strain. In addition, the grains in which the *c*-axis is largely tilted toward the TD (e.g. the circled area in Fig. 2(a)) tend to show higher IQs, indicating relatively lower dislocation densities compared with the basal oriented grains. For the specimen annealed at 573 K for 5 s, some bright, small, and equiaxial grains with grain sizes of 1–5 μm are observed and the fraction of low angle grain boundaries (LAGB) also decreases correspondingly, indicating the beginning of SRX. Annealing at 623 K for 10 s reduces the fraction of the LAGB to a quite low level and the twins also disappear, indicating the completion of SRX. The basal texture is significantly weakened at this annealing stage. Severe annealing at 773 K for 3.6×10^3 s results in significant grain growth from 9 μm to 23 μm (measured using EBSD) and a further weakening of the basal texture, accompanied by an enhancement of the basal pole inclination. These tendencies are consistent with those of the macro textures, as shown in Fig. 1. The $\langle 10\bar{1}0 \rangle$ direction tends to be oriented parallel to the RD, and this orientation is retained even after severe annealing, indicating that the change in the *c*-axis orientation is the major feature of texture evolution. With the exception of the specimen annealed at 773 K for 3.6×10^3 s, all the specimens exhibit a dominant misorientation angle of high angle grain boundaries (HAGB) at ~30°, which is typically found for Mg alloy sheets with a strong basal texture [23]. The fraction of the HAGB larger than 30° is significantly increased upon the completion of SRX, which contributes to the weakening of the texture, however, the peak at ~30° persists (see Fig. 2(c)). In contrast, severe annealing results in a significant shift of the peak of the misorientation angle

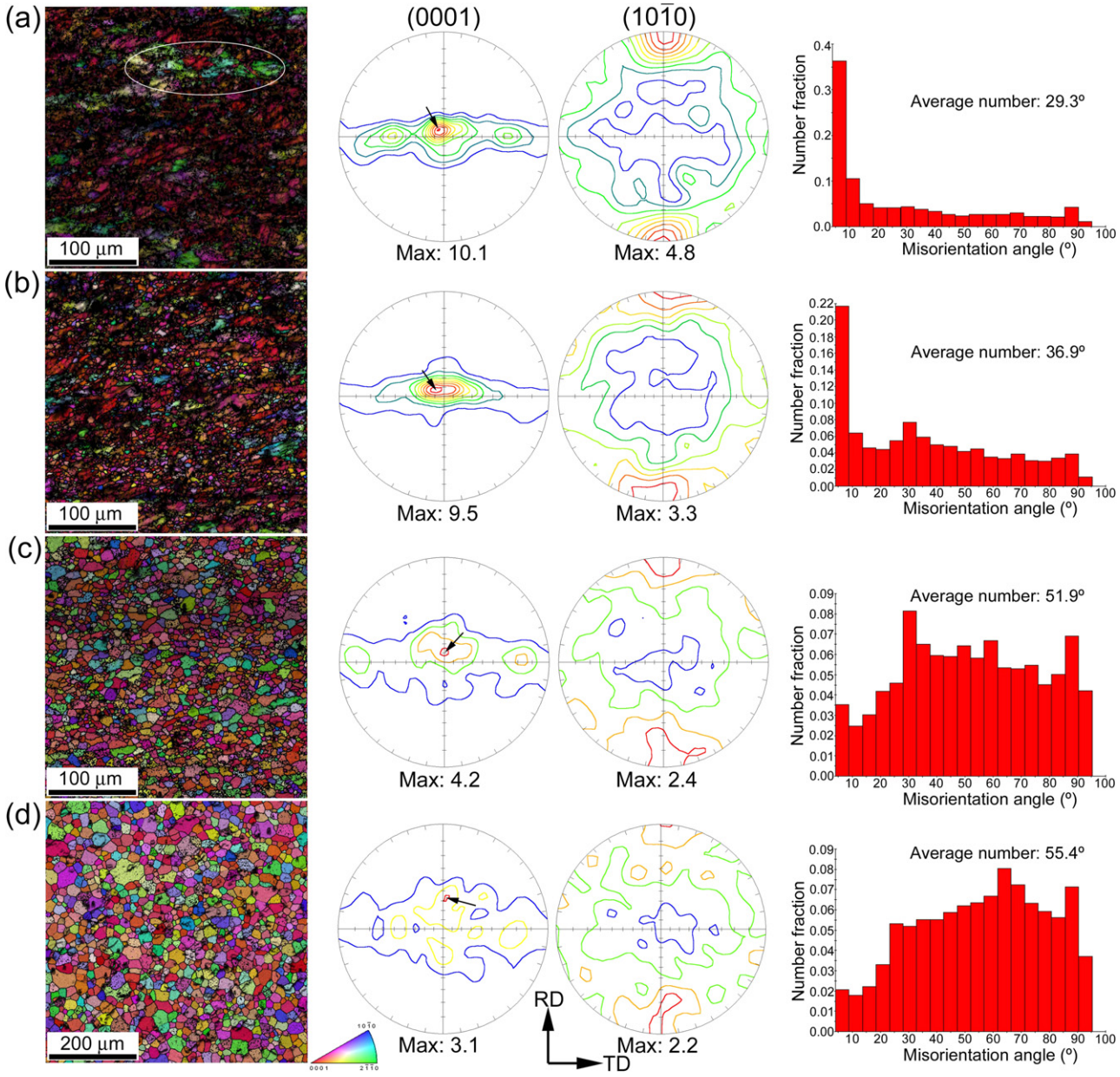

Fig. 2. Inverse pole figure maps with horizontal RD, (0 0 0 1) pole figures (intensity levels: 1, 2, 3, etc.), (1 0 $\bar{1}$ 0) pole figures (intensity levels: 0.5, 1, 1.5, etc.) and distributions of grain boundary misorientation of (a) as-rolled sheet together with sheets annealed at (b) 573 K for 5 s, (c) 623 K for 10 s, and (d) 773 K for 3.6×10^3 s, measured using EBSD. Compared with the other specimens with an analyzed area of 9×10^4 μm^2, the specimen severely annealed at 773 K for 3.6×10^3 s was analyzed at a larger area of 3.6×10^5 μm^2 because of its much larger grain size. The arrows indicate the maxima of the (0 0 0 1) pole figures.

to 60–65°, which accompanies severe grain coarsening after the completion of SRX (see Fig. 2(d)).

As shown in Fig. 3(a), the textures associated with the grains smaller than 5 μm and larger than 10 μm, which mainly correspond to the new SRXed and non-recrystallized grains, respectively, were extracted from the texture of the specimen annealed at 573 K for 5 s with the initial state of SRX (see Fig. 2(b)). The new SRXed grains exhibit dispersed orientations and a significantly weakened basal texture owing to the considerable change in the *c*-axis orientation from the initial basal orientation compared with the non-recrystallized grains.

In order to obtain more detailed information on texture evolution during grain growth after the completion of SRX, the grains were separated into two categories: smaller than and larger than the average grain size. Figs. 3(b–d) show the textures of the grains smaller than or larger than 9 μm, 12 μm, and 23 μm, which are the average grain sizes for the specimens annealed at 623 K for 10 s, 623 K for 3.6×10^3 s, and 773 K for 3.6×10^3 s, respectively. All the textures of the smaller grains exhibit the inclination of the basal pole toward the RD. These textures are similar to that associated with the new SRXed grains primarily appearing at the initial stage of annealing (see Fig. 3(a)). In contrast, the maxima tend to be distributed in the TD for the textures of the larger grains. This may be due to a larger stored energy for the basal oriented grains compared with those in which the *c*-axis is largely tilted toward the TD, as indicated by the different IQs for the grains belonging to the two texture components (see Fig. 2(a)). The textures of both the smaller and the larger grains weaken as grain coarsening progresses. This weakening is especially pronounced for the smaller grains. The texture of the smaller grains exhibits a large decrease in the basal texture intensity from 5.7 to 4.1, whereas the intensity for the larger grains drops from 5.0 to 4.3. In addition, it is obvious

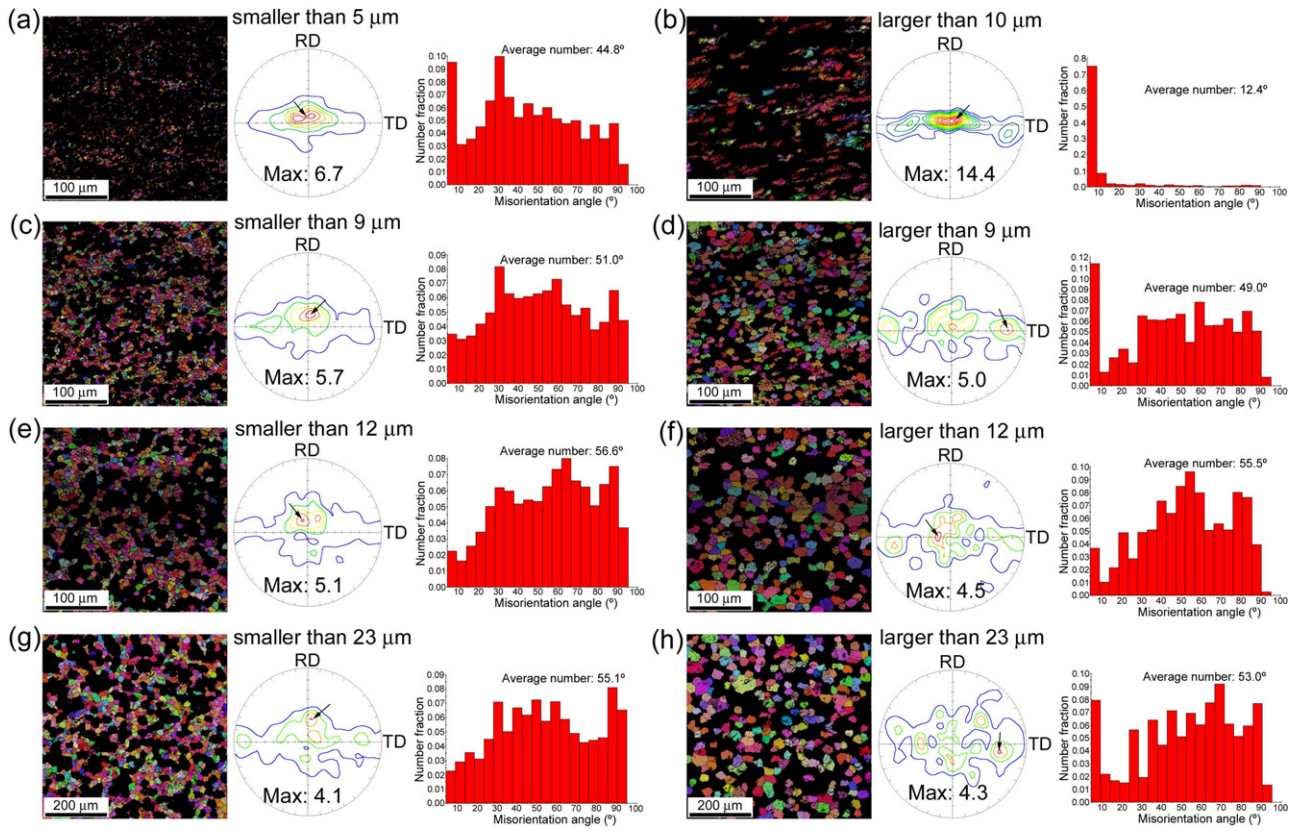

Fig. 3. Inverse pole figure maps, (0 0 0 1) pole figures (intensity levels: 1, 2, 3, etc.), and distributions of grain boundary misorientation of (a, c, e, and g) smaller grains (left part) and (b, d, f, and h) larger grains (right part) in sheets annealed at (a and b) 573 K for 5 s, (c and d) 623 K for 10 s, (e and f) 623 K for 3.6×10^3 s, and (g and h) 773 K for 3.6×10^3 s, measured using EBSD. The arrows indicate the maxima of the (0 0 0 1) pole figures.

that the inclination of the basal pole toward the RD originates from the smaller grains and the grain growth of the smaller grains leads to the enhancement of the basal pole inclination. For the specimen treated under severe annealing conditions at 773 K for 3.6×10^3 s, the grains with a size less than 23 μm and an average grain size of 16 μm are further separated into grains smaller or larger than 16 μm, as shown in Fig. 4. The texture associated with the larger grains (16–23 μm) exhibits a greater inclination of the basal pole,

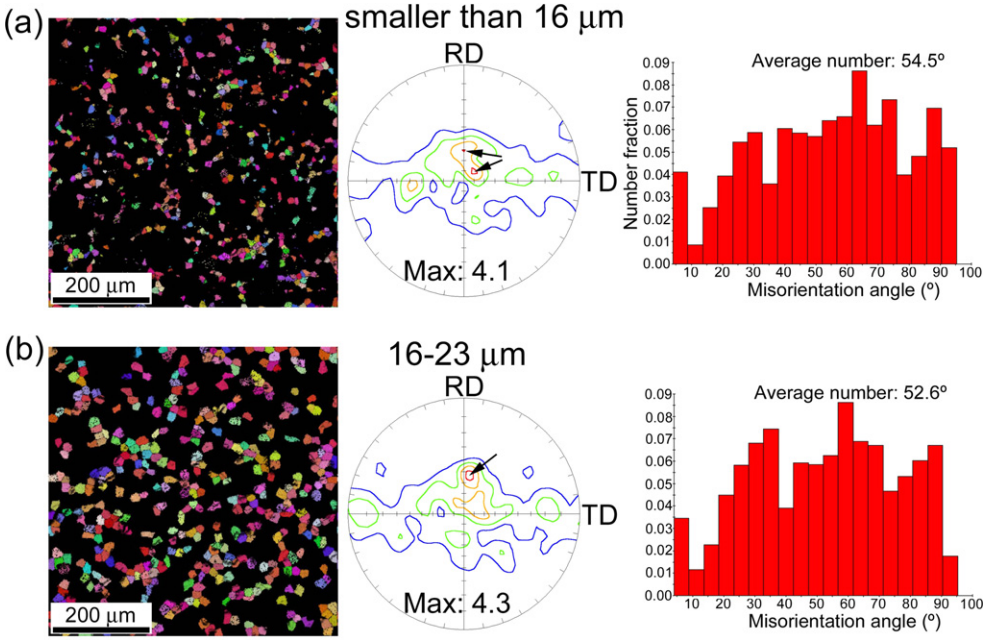

Fig. 4. Inverse pole figure maps, (0 0 0 1) pole figures (intensity levels: 1, 2, 3, etc.), and distributions of grain boundary misorientation of (a) smaller grains with grain sizes smaller than 16 μm and (b) larger grains with grain sizes of 16–23 μm in sheets annealed at 773 K for 3.6×10^3 s, measured using EBSD. The arrows indicate the maxima of the (0 0 0 1) pole figures.

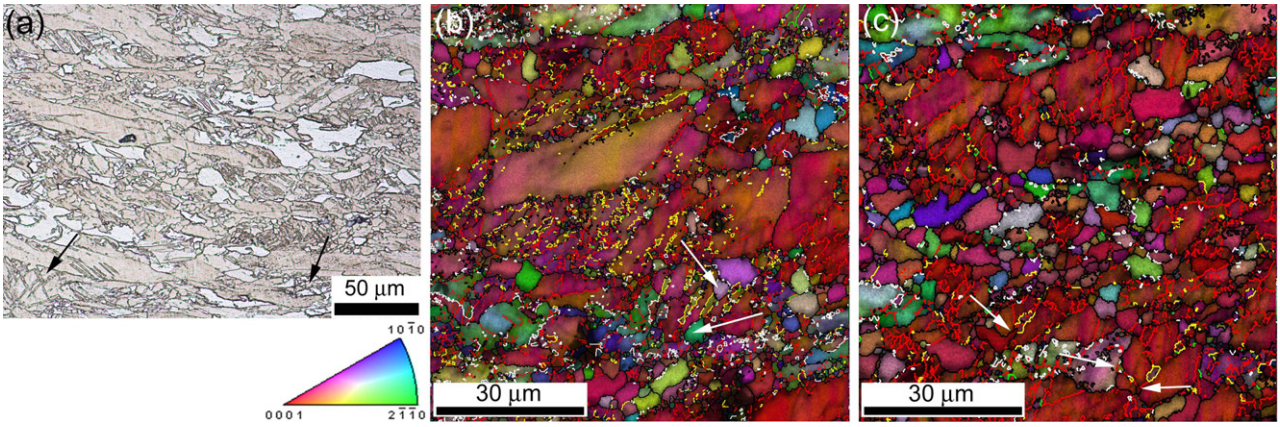

Fig. 5. (a) Optical micrograph and (b and c) inverse pole figure maps of two different areas in specimen annealed at 573 K for 5 s, measured using EBSD at fine step sizes of 0.2–0.3 μm. HAGB (>15°), LAGB (4–15°), boundaries of tensile, compression, and double twins are characterized by black, red, white, green, and yellow lines, respectively. (For interpretation of the references to color in this sentence, the reader is referred to the web version of the article).

indicating preferential growth of the grains with the *c*-axis largely tilted toward the RD.

As mentioned above, the main peak of the misorientation angle is significantly shifted from ~30° to 60–65° following grain coarsening, which occurs under severe annealing conditions. The reason for this phenomenon is not yet clear. Among the limited literature on the relationship between grain boundary energy and misorientation angle for pure Mg, it has been reported, on the basis of molecular dynamics simulation, that the grain boundary energy of the $[1\,\bar{1}\,0\,0]$ symmetric tilt boundary decreases gradually as the misorientation angle increases and becomes stable at ~60° with apparent drops near the misorientation angles of twin boundaries [24]. Therefore, it is suggested that grain rotation that increases the misorientation angle and thereby lowers the grain boundary energy and/or preferential growth of the grains having large misorientation angles might occur during grain coarsening, thus contributing to the weakening of the texture. A similar possibility of the formation of preferential misorientations related to coincidence site lattices during grain growth in a deformed and subsequently annealed zirconium alloy has also been pointed out by Zhu et al. [25]. The greater weakening of the texture associated with the smaller grains may be explained by the preference for the smaller grains for grain rotation during grain coarsening.

Fig. 5 shows the optical micrograph and the inverse pole figure maps measured at two different areas of the specimen annealed at 573 K for 5 s with the initial state of SRX. The fractions of 86° $\{1\,0\,\bar{1}\,2\}$ tensile, 56° $\{1\,0\,\bar{1}\,1\}$ compression, and 38° $\{1\,0\,\bar{1}\,1\} - \{1\,0\,\bar{1}\,2\}$ double twins are 6%, 1%, and 3%, respectively. Compression twinning and double twinning occur in the grains belonging to the basal fiber as a result of the favoured orientation for increasing the compression stress component along the *c*-axis during rolling. Conversely, tensile twinning occurs mainly in the grains with non-basal orientations. The largest fraction of the tensile twins can be attributed to the relatively weak basal texture prior to final warm rolling and the lowest critical resolved shear stress among twinning systems. The new grains nucleate mostly at the pre-existing grain boundaries rather than at the intersections of twins or within the twins (see arrows in Fig. 5(a)) owing to discontinuous SRX. In spite of the large number of twins in the deformed grains, this phenomenon is different from the previously reported twin-related SRX, in which the new grains mostly formed at the intersections of twins or within the twins [8–10,26,27]. The new grains around the grain boundaries tend to exhibit a largely altered *c*-axis orientation away from the basal orientation, leading to significant weakening of the basal texture.

Nucleation at the grain boundaries during annealing has also been observed in hot compressed Mg–Mn alloy with an initial cast structure as well as in cold deformed AZ31 alloy [13,28]. There are two possible mechanisms responsible for this phenomenon. Firstly, it is known that the grain boundaries result in inhomogeneous deformation and non-basal slips may be activated near the grain boundaries to relieve strain incompatibilities [29–31]. This induces large orientation gradients and large local dislocation densities with dislocations on various slip planes in the vicinity of the pre-existing grain boundaries, which provide favoured nucleation sites and may result in new grains with a random orientation [30,31]. Another possibility is strain induced grain boundary migration (SIBM), as indicated by the serrated pre-existing grain boundaries (see Fig. 5), which has also been observed and reported in Ref. [13]. The driving force for SIBM usually arises from a difference in the dislocation content on opposite sides of the grain boundary and results in bulging from a grain with a lower stored energy toward a grain with a higher one [31]. The microstructure of the as-rolled sheet is quite heterogeneous as shown in Fig. 6. The dislocation densities inside the grains are quite different even among the large elongated grains that are free of twins, suggesting a slip dominated deformation (see Figs. 6(a and b)). This may be attributed to the relatively weak basal texture prior to final warm rolling, which leads to different Schmid factors for basal slip and thus different deformation capabilities among the individual grains. In addition, the grain that contains twins appears to have a relatively low dislocation density (see Fig. 6(c)), which suggests that the grains deformed by twinning less accommodate external strain by the slip dominated mechanism. Moreover, the parent grains may be almost completely consumed by the tensile twins due to the ease of operation [9]. The large grains that are reoriented by tensile twinning undergo a relatively low level of deformation to accommodate external strain [32], which lowers the dislocation densities of those grains that appear to be free of twins. Moreover, the thin double twins may form in the newly reoriented grains generated by tensile twinning [33]. The extensive twinning is thus beneficial for enhancing the heterogeneity of the microstructure. Therefore, it can be considered that SIBM may be induced by the heterogeneity of the microstructure with different dislocation densities among the deformed grains, which originates from the microstructure of the sheet hot rolled at 823 K exhibiting a relatively weak texture and coarse grains prior to final warm rolling. However, the new grains induced by SIBM are generally characterized by similar orientations with respect to the parent grains from which they have grown [31]. Nucleation of some new grains with a largely altered *c*-axis orientation is observed at the

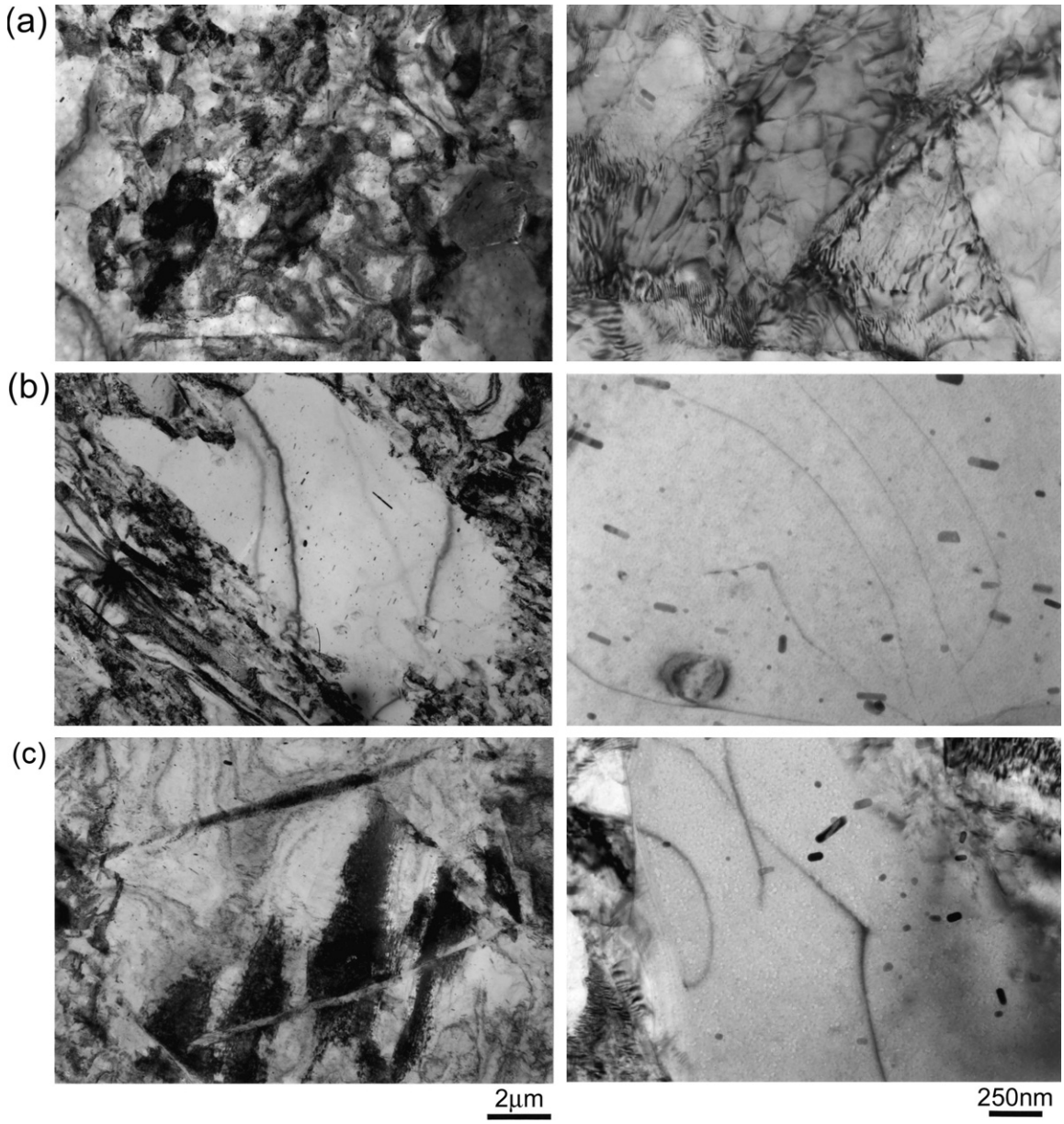

Fig. 6. TEM images of three types of large elongated grains in as-rolled sheet: two grains free of twins with (a) high and (b) low dislocation densities. (c) Grain containing twins with low dislocation density, observed at low (left part) and high (right part) magnifications.

border between the double twins and the pre-existing grain boundaries (see arrows in Fig. 5(b)). The bulging of the pre-existing grain boundaries from the adjacent grains toward the double twins is also observed (see arrows in Fig. 5(c)). This bulging occurs because the double twins generally have higher dislocation densities, as indicated by their lower IQs, compared with the parent grains (see Fig. 5(b and c)) owing to its preferred orientation for the basal slip. These observations indicate the possibility that the new grains might be induced by the SIBM mechanism followed by rotation, if the bulging is considered to be an early stage of SRX. Therefore, it is postulated that the rotation of the *c*-axis occurs in order to lower the grain boundary energy, as mentioned above, and/or as a result of the absorption of the non-basal dislocations near the pre-existing grain boundaries after nucleation. Future work observing the microstructural and textural evolution in the same area may provide further information on whether the new grains rotate after nucleation and which mechanism dominates the texture randomization.Even though the direct contribution of twins to the texture randomization during SRX appears to be low, it should be emphasized that twinning plays an important role in the restriction of DRX and in the enhancement of the heterogeneity of the microstructure during final warm rolling [20]. It is well known that the addition of RE elements has a remarkable effect on the weakening of the texture of Mg alloys. Hantzsche et al. [23] demonstrated that this weakening of the texture is related to the presence of deformation bands containing twins as well as the restriction of grain growth because of grain boundary pinning effects caused by solute segregation or particles during annealing. In contrast, the present work shows that discontinuous SRX occurring at the grain boundaries can lead to a significantly weakened texture even after severe grain coarsening in the typical Mg alloy (AZ31) without the addition of RE elements. This grain growth behaviour is somewhat different from that generally observed in hexagonal metals, in which the grain growth often results in a tex-

ture evolution corresponding to a ∼30° rotation around the *c*-axis [25,34].

4. Conclusions

In summary, the AZ31 alloy sheet obtained by a combination of high-temperature rolling and subsequent warm rolling exhibits a different annealing behaviour from that which is generally observed in Mg alloys. The microstructure of the as-rolled sheet is quite heterogeneous and contains a large number of deformation twins. The new grains nucleate mostly at the pre-existing grain boundaries rather than at the intersections of the twins or within the twins during primary recrystallization. The new grains formed by discontinuous SRX tend to exhibit a *c*-axis orientation that is largely altered from the initial basal orientation and, in turn, leads to a significant weakening of the basal texture. Further progression of the texture weakening, accompanied by the enhancement of the basal pole inclination, occurs during the subsequent grain growth even after severe grain coarsening.

References

[1] G.R. Ebrahimi, A.R. Maldar, R. Ebrahimi, A. Davoodi, J. Alloys Compd. (2010) doi:10.1016/j.jallcom.2010.11.134.
[2] A. Galiyev, R. Kaibyshev, G. Gottstein, Acta Mater. 49 (2001) 1199.
[3] X.Y. Yang, H. Miura, T. Sakai, Mater. Trans. 46 (2005) 2981.
[4] X.Y. Yang, Y.K. Zhu, H. Miura, T. Sakai, Trans. Nonferrous Met. Soc. China 20 (2010) 1269.
[5] L.W.F. Mackenzie, M. Pekguleryuz, Mater. Sci. Eng. A 480 (2008) 189.
[6] X.S. Huang, K. Suzuki, A. Watazu, I. Shigematsu, N. Saito, J. Mater. Res. 23 (2008) 3029.
[7] S. Abdessameud, D. Bradai, Can. Metall. Quart. 48 (2009) 433.
[8] É. Martin, L. Jiang, S. Godet, J.J. Jonas, Int. J. Mat. Res. 100 (2009) 576.
[9] S.B. Yi, I. Schestakow, S. Zaefferer, Mater. Sci. Eng. A 516 (2009) 58.
[10] X. Li, P. Yang, L.N. Wang, L. Meng, F. Cui, Mater. Sci. Eng. A 517 (2009) 160.
[11] S.R. Wang, M. Wang, S.B. Kang, J.H. Cho, Trans. Nonferrous Met. Soc. China 20 (2010) 763.
[12] H.M. Chen, H.S. Yu, S.B. Kang, J.H. Cho, G.H. Min, Mater. Sci. Eng. A 527 (2010) 1236.
[13] J.D. Robson, D.T. Henry, B. Davis, Acta Mater. 57 (2009) 2739.
[14] E.A. Ball, P.B. Prangnell, Scripta Metall. Mater. 31 (1994) 111.
[15] S.A. Torbati-Sarraf, R. Mahmudi, Mater. Sci. Eng. A 527 (2010) 3515.
[16] M. Huppmann, S. Gall, S. Müller, W. Reimers, Mater. Sci. Eng. A 528 (2010) 342.
[17] A.G. Beer, M.R. Barnett, Metall. Mater. Trans. A 38A (2007) 1856.
[18] Y. Chino, K. Sassa, M. Mabuchi, Mater. Sci. Eng. A 513–514 (2009) 394.
[19] D. Wu, R.S. Chen, E.H. Han, J. Alloys Compd. (2010) doi:10.1016/j.jallcom.2010.11.141.
[20] X.S. Huang, K. Suzuki, N. Saito, Scripta Mater. 61 (2009) 445.
[21] X.S. Huang, K. Suzuki, N. Saito, Scripta Mater. 60 (2009) 651.
[22] X.S. Huang, K. Suzuki, A. Watazu, I. Shigematsu, N. Saito, J. Alloys Compd. 457 (2008) 408.
[23] K. Hantzsche, J. Bohlen, J. Wendt, K.U. Kainer, S.B. Yi, D. Letzig, Scripta Mater. 63 (2010) 725.
[24] J.T. Chou, K.I. Ikeda, H. Nakashima, J. Japan Inst. Met. 69 (2005) 303.
[25] K.Y. Zhu, B. Bacroix, T. Chauveau, D. Chaubet, O. Castelnau, Metall. Mater. Trans. A 40A (2009) 2423.
[26] A. Jäger, P. Lukáč, V. Gärtnerová, J. Haloda, M. Dopita, Mater. Sci. Eng. A 432 (2006) 20.
[27] J.Z. Liu, T.M. Liu, H. Yuan, X.L. Shi, Z.C. Wang, Mater. Trans. 51 (2010) 341.
[28] C.W. Su, L. Lu, M.O. Lai, Philos. Mag. 88 (2008) 181.
[29] J. Koike, T. Kobayashi, T. Mukai, H. Watanabe, M. Suzuki, K. Maruyama, K. Higashi, Acta Mater. 51 (2003) 2055.
[30] M. Hasegawa, H. Fukutomi, Mater. Trans. 43 (2002) 2243.
[31] F.J. Humphreys, M. Hatherly, Recrystallization and Related Annealing Phenomena, second ed., Pergamon, Oxford, 2004.
[32] S.-H. Choi, D.H. Kim, B.S. Seong, Met. Mater. Int. 15 (2009) 239.
[33] Z. Zhang, M.P. Wang, N. Jiang, S.M. Li, Mater. Sci. Eng. A 527 (2010) 6467.
[34] N. Bozzolo, F. Wagner, N. Dewobroto, T. Grosdidier, Mater. Sci. Forum 408–412 (2002) 901.